THE JOURNAL OF PHYSICAL CHEMISTRY B

Article

pubs.acs.org/JPCB

Revisiting the Aqueous Solutions of Dimethyl Sulfoxide by Spectroscopy in the Mid- and Near-Infrared: Experiments and Car–Parrinello Simulations

Victoria M. Wallace,[†] Nilesh R. Dhumal,[‡] Florian M. Zehentbauer,[§] Hyung J. Kim,[‡,⊥] and Johannes Kiefer*[,†,§,∥]

[†]School of Engineering, University of Aberdeen, Fraser Noble Building, Aberdeen AB24 3UE, United Kingdom

[‡]Department of Chemistry, Carnegie Mellon University, Pittsburgh, Pennsylvania 15213, United States

[§]Technische Thermodynamik, Universität Bremen, Badgasteiner Str. 1, 28359 Bremen, Germany

[∥]Erlangen School of Advanced Optical Technologies (SAOT), Universität Erlangen-Nürnberg, Erlangen, Germany

[⊥]School of Computational Sciences, Korea Institute for Advanced Study, Seoul 130-722, Korea

Supporting Information

ABSTRACT: The infrared and near-infrared spectra of the aqueous solutions of dimethyl sulfoxide are revisited. Experimental and computational vibrational spectra are analyzed and compared. The latter are determined as the Fourier transformation of the velocity autocorrelation function of data obtained from Car–Parrinello molecular dynamics simulations. The experimental absorption spectra are deconvolved, and the excess spectra are determined. The two-dimensional excess contour plot provides a means of visualizing and identifying spectral regions and concentration ranges exhibiting nonideal behavior. In the binary mixtures, the analysis of the SO stretching band provides a semiquantitative picture of the formation and dissociation of hydrogen-bonded DMSO–water complexes. A maximum concentration of these clusters is found in the equimolar mixture. At high DMSO concentration, the formation of rather stable 3DMSO:1water complexes is suggested. The formation of 1DMSO:2water clusters, in which the water oxygen atoms interact with the sulfoxide methyl groups, is proposed as a possible reason for the marked depression of the freezing temperature at the eutectic point.

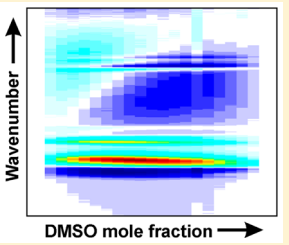

1. INTRODUCTION

The binary mixtures of the polar aprotic solvent dimethyl sulfoxide (DMSO) and water have been a very active and fascinating field of research for many decades.[1] One of the main reasons is that mixtures of DMSO and water exhibit highly nonideal thermodynamic and transport behaviors.[2,3] For example, mixtures consisting of 1DMSO:3water exhibit intriguing properties (e.g., viscosity) that are not straightforward to understand.[4,5] Perhaps the most prominent nonideality is the freezing point which decreases to as low as −70 °C at the eutectic point at the molar ratio 1DMSO:2water.[6,7] This is remarkable in that the freezing points of the pure liquids are +18 and 0 °C, respectively. A detailed overview can be found in ref 1. Because of their interesting and unique properties, aqueous DMSO solutions are not only a matter of academic curiosity but also important materials commonly used as solvents, antifreeze fluids, and cryo-protectants.[8]

The macroscopic peculiarities arise from the behavior at the molecular level. It is commonly accepted that the molecular behavior is governed by hydrogen bonds between DMSO and water molecules leading to enhanced polarizations in the molecules.[9−11] However, a universal physical theory of the mutual solvation is yet to be found. Numerous theoretical and experimental studies have been carried out in order to unravel the phenomena observed. For example, Kirchner et al. performed Car–Parrinello simulations for analyzing the structure of a DMSO–water mixture.[12] Most models assume that hydrogen-bond formation starts with the DMSO oxygen and water hydrogen atoms, which act as electron donor and proton donor, respectively. On the other hand, water molecules can interact with the methyl hydrogen atoms, which is often referred to as hydrophobic hydration.[13] In order to explain this phenomenon, Mizuno et al.[14,15] proposed the "push ball" hydration mechanism, where the water molecules experience a polarization increase because of their initial interactions with the sulfoxide group. This results in an enhanced hydrogen-bond acceptor ability, which enables the interaction with the DMSO methyl hydrogen atoms via electronic repulsion or dispersion. Mrazkova and Hobza[16] proposed a different explanation. They introduced the theory of progressive hydration. In this model, the first part of the hydration shell is formed around the sulfoxide group, which is eventually saturated with hydrogen bonds. Subsequently, the hydration shell is completed by hydrogen bonds between the DMSO methyl hydrogen and water oxygen atoms. Li et al.[17−19] followed a similar line of argument in their cooperativity model. A complete picture,

Received: September 21, 2015
Revised: October 23, 2015
Published: October 28, 2015

DOI: 10.1021/acs.jpcb.5b09196
J. Phys. Chem. B 2015, 119, 14780−14789

however, is yet to be developed and hence the need for additional theoretical and experimental analysis that will allow new and complementary information to be obtained.

In the present paper, we investigate the potential of using spectroscopy in the mid- and near-infrared spectral range to gain new insights into aqueous DMSO solutions in the entire composition range from pure water to pure DMSO. The IR spectrum is frequently employed for this purpose, and thus it is used here as a reference. Novel aspects of our work from the methodology perspective include the analysis of the DMSO combination bands in the NIR spectrum and the utilization of the excess spectra in the extended spectral range. In order to provide an unambiguous interpretation of the results, additional experiments are performed with the deuterated form of DMSO, DMSO-d_6. Furthermore, a few select mixtures have been studied using *ab initio* molecular dynamics simulations to obtain the computational vibrational spectra. The outline of this paper is as follows: Sections 2 and 3 describe the experimental and computational methods, respectively. Section 4 presents the results along with their interpretation: First, the spectra of the pure solvents are discussed. The spectra of the mixtures and their frequency shifts are analyzed next. Lastly, excess spectra are examined. Section 5 concludes.

2. EXPERIMENTAL METHOD

Dimethyl sulfoxide of purity 99.9% was used to make solutions of DMSO/water, from pure water to pure DMSO, in steps of $\Delta x_{DMSO} = 0.05$, where x_{DMSO} is the mole fraction of DMSO. The mole fractions of DMSO were converted to mass and measured out using an analytical balance. The measured DMSO was topped up with water to a total mass of 3 g. A purification system delivered deionized water with a resistivity of 18.2 MΩ·cm. In addition, binary mixtures of water and DMSO-d_6 (99.96 atom %) were prepared in steps of $\Delta x_{DMSO\text{-}d_6} = 0.1$.

A Bruker Vertex 70 FTIR spectrometer equipped with an ATR accessory (diamond, 1 reflection, 45°) was used to collect the absorption spectra. For the mid-IR spectral range, 16 scans with a nominal resolution of 1 cm^{-1} in the range from 500 to 4000 cm^{-1} were averaged. In the near-IR range, 128 scans with a resolution of 4 cm^{-1} were averaged over the range from 3900 to 7000 cm^{-1}. The higher number of scans was necessary in order to obtain a sufficient signal-to-noise ratio due to the weak absorption of the overtone and combination bands and the lower ATR penetration depth in the NIR. All measurements were carried out at room temperature (294 K) and pressure. In order to avoid changes in the sample composition due to selective evaporation of one component, the sample was covered with a glass cap during the measurement.

For data analysis, key regions of the IR spectra were evaluated using summed Gaussian profiles in order to track the movement of superimposed peaks. For this purpose, a Matlab routine based on a least-squares fit was employed. We note that such a fitting of profiles needs to be done with care, as it can result in data without a physical meaning. Here, we have preset the number of profiles and prescribed appropriate ranges of their center frequency and line width, while the intensity was an unconditioned fitting parameter. The determination of these boundary conditions took into account the experimental data (e.g., derivative spectra), instrument parameters (e.g., resolution), and experience from previous work as well as information from the literature. Finally, the peak shifts were calculated relative to the pure peak frequencies and plotted against the DMSO mole fraction. The excess spectra were calculated as described in the literature[20−22] and in previous work by Kiefer and co-workers.[23−26]

3. COMPUTATIONAL METHOD

A vibrational analysis can also be performed using computational methods. There are at least two different approaches for calculating the vibrational spectrum: (1) The normal modes can be obtained by diagonalization of the Hessian matrix evaluated by computing the second derivative of the potential surface. (2) A more systematic approach is calculating the vibrational density of the states from a molecular dynamics (MD) simulation by Fourier transformation of the dipole moment autocorrelation function.[27−29] With the neglect of dipole moment variations with positions, e.g., bond lengths, the IR absorption can be further simplified as Fourier transformation of the velocity autocorrelation function[30] (VAF):

$$I(\omega) = \frac{4\pi\beta}{3cV}\int_0^\infty c(t)\cos(\omega t)\,\mathrm{d}t \quad \text{with } c(t) = \langle v(t_0 + t)\cdot v(t_0)\rangle \tag{1}$$

where $\langle\ \rangle$ is the equilibrium ensemble average. We have two remarks: First, since dipole fluctuations of the system relevant to IR absorption are approximated as position (and thus velocity) fluctuations of individual atoms in eq 1, its predictions for peak intensities are not as accurate as those for peak positions. Second, the prefactor in eq 1 depends on how one corrects the dipole time correlation function based on classical nuclear dynamics, so that it meets the detailed balance condition. Different correction methods will yield different prefactors.[31]

In the present study, an *ab initio* molecular dynamics (Car−Parrinello[32]) simulation was conducted for DMSO/water mixtures at five different compositions using the CPMD program (version 3.17.1).[33] These include the pure DMSO and water cases as well as three binary systems covering the low DMSO concentration range up to approximately the eutectic point. The corresponding numbers of water and DMSO molecules the density values employed in the simulations are summarized in Table 1.

Table 1. Details of Simulated Mixtures

mole fraction of DMSO	no. of DMSO molecules	no. of water molecules	density (g cm^{-3})
0	0	64	1.024
0.10	5	43	1.035
0.20	8	32	1.067
0.31	10	22	1.046
1	16	0	1.100

The initial configurations used in the CPMD simulations were obtained from classical MD simulations of 10 ns duration. Three-dimensional periodic boundary conditions were imposed on the cubic box of edge length 12.32 Å. In the DFT framework, we use the Becke−Lee−Yang−Parr[34,35] BLYP functional to treat the exchange-correlation interaction between electrons, which has been shown to give a good description of the vibrational properties. The interaction between the core and the valence electrons is described by the Troullier−Martins norm-conserving pseudopotential.[36] The electronic orbitals

DOI: 10.1021/acs.jpcb.5b09196
J. Phys. Chem. B 2015, 119, 14780−14789

were expanded in a plane wave basis set with an energy cutoff of 80 Ry.[37]

Car−Parrinello molecular dynamics simulations were performed in the NVT ensemble at 300 K for 16.0 ps after 4 ps equilibration. The fictitious orbital mass was set at 400 au, and the equations of motion were integrated with a time step of 4 au = 0.097 fs. We remedied the lack of van der Waals interactions by invoking an effective dispersion-correction.[38]

4. RESULTS AND DISCUSSION

4.1. IR and NIR Spectrum of the Pure Solvents. The experimental IR and NIR spectra of pure water and DMSO are displayed in Figure 1a. It is well-known that the mid-IR

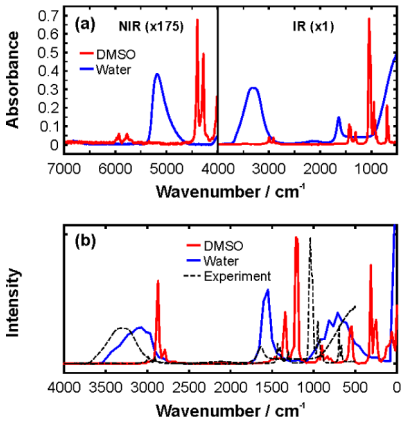

Figure 1. (a) Experimental absorption spectrum in the mid- and near-IR of water and DMSO at room temperature. The NIR spectra are multiplied by a factor of 175 in order to be of comparable absorbance. (b) Computational vibrational spectrum of water and DMSO obtained from the Fourier transformation of the velocity autocorrelation function. The dashed lines in (b) represent the experimental IR data from panel (a) for a better comparison.

spectrum mainly comprises the fundamental vibrational modes while the NIR region contains overtone and combination bands. We first consider the water case. Its IR spectrum is dominated by broad bands, where the most prominent features are the OH bending mode peaking at 1636 cm^{-1} and the broad OH stretching band ranging from 2800 to 3700 cm^{-1}. The computational water spectrum obtained by Fourier transform of the VAC, eq 1, is shown in Figure 1b. The OH stretching frequency in the simulation spectra is predicted to be in the range 2750−3600 cm^{-1}, whereas the vibration at 1600 cm^{-1} is assigned to the OH bending mode. These assignments agree well with the experimental IR spectrum including the band shapes and widths. Nevertheless, the main peak positions of the computational spectrum are slightly red-shifted compared to the experimental results.

In the NIR range shown in Figure 1a, the only significant absorption band of water is the asymmetric band with its peak at 5180 cm^{-1}. It can be assigned to the combination of the OH bending and stretching vibrations. This band has been utilized in a recent study of DMSO/water solutions. Specifically, Klemenkova and Kononova[39] analyzed the dependence of its position and shape on DMSO concentration. However, since the fundamental OH stretching band is rich in information and little affected by DMSO signals, we will use the stretching band for further analysis and discussion in the subsequent sections. For completeness, we note that the overtones of the OH stretching modes appear as a very weak band between 6500 and 7000 cm^{-1} in Figure 1a. A detailed analysis of this band was reported by Bertoluzza et al.[40] They performed measurements in transmission using a sample thickness of 1 mm in order to obtain an appropriate signal-to-noise ratio. The ATR experiment used in the present work is not as sensitive, and thus we will not consider this band here anymore.

Returning to the fundamental OH stretching band, in order to extract detailed information, this band has been deconvolved as a sum of Gaussian profiles as displayed in Figure 2. For

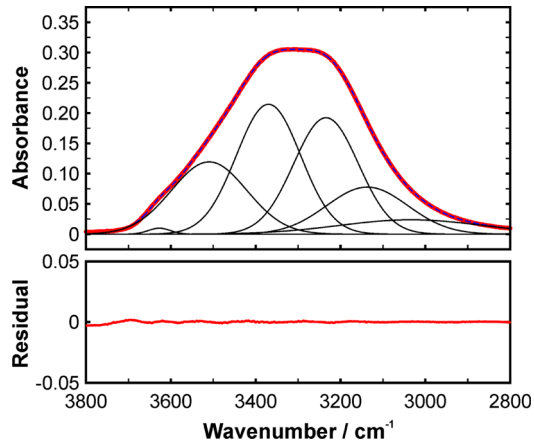

Figure 2. OH stretching band of liquid water. The thick red curve shows the experimental spectrum, and the dashed line represents a best-fit function based on six individual Gaussian profiles, which are displayed as thin solid lines. The lower panel shows the residual between the fitted curve and the experimental data.

consistency with previous work, six individual Gaussian profiles were used. The fit yielded peak positions at 3629, 3533, 3389, 3241, 3139, and 3045 cm^{-1}, which is in good agreement with previous results of Kiefer and co-workers[41] and of Schmidt and Miki.[42] The different peaks can be assigned to water molecules in different hydrogen-bonded states; i.e., the lower the frequency, the more intense the hydrogen-bonding interaction.[42]

The DMSO spectra exhibited in Figure 1 show more pronounced features than water. At the low-frequency end of the experimental data, the symmetric and antisymmetric CSC stretching vibrations are present at 667 and 697 cm^{-1}, respectively. The corresponding band centered at 570 cm^{-1} in the simulation spectrum is red-shifted by ∼110 cm^{-1} compared to the experimental result. The peak at 952 cm^{-1} with the corresponding computational structure at 920 cm^{-1} can be assigned to CH bending. Additional CH bending modes are located at 1310 and 1407 cm^{-1}, while the band at 1230 cm^{-1} in the simulated spectrum is attributed to these vibrations. The structures associated with symmetric and antisymmetric CH stretching modes can be found at 2912 and 2996 cm^{-1}, respectively.

The dominating absorption band in the mid-IR is the SO stretching mode. This band is located at around 1042 cm^{-1} in the experimental data, while it appears at 1375 cm^{-1} in the simulation. For a detailed analysis, this band in the experimental spectra was fitted by four individual Gaussian profiles. The results for their center frequencies are 1019, 1031, 1041, and 1052 cm^{-1}. The peaks at 1041 and 1052 cm^{-1} can be assigned to the stretching of the S═O bond.[43] In this context it is worthwhile to note that DMSO can form chain-like and cyclic

DOI: 10.1021/acs.jpcb.5b09196
J. Phys. Chem. B 2015, 119, 14780−14789

structures via polar interactions of the sulfoxide groups.[44−46] We attribute the peak at 1052 cm^{-1} to those DMSO molecules not participating in the self-association, while the red-shifted peak at 1041 cm^{-1} is attributed to self-associated DMSO. The peaks at 1019 and 1031 cm^{-1} correspond to rocking vibrations of the methyl groups. This assignment is supported by the DMSO-d_6 spectra, in which the SO modes can be observed at very similar wavenumbers while the CD_3 modes are shifted due to the different mass of deuterium compared to hydrogen.

The superimposed IR spectra in the right part of Figure 1a reveal that there are basically no DMSO peaks, which do not overlap with strong and broad water bands. Hence, the analysis and interpretation of the mixture IR spectra are challenging. This situation changes in the NIR, which makes this range a potentially interesting alternative that deserves consideration. The main features of the DMSO NIR spectrum are the strong peaks at 4279 and 4397 cm^{-1}. They are spectrally separated from water bands. Although this region of the NIR spectrum of DMSO has been reported and analyzed, unambiguous assignments of its bands have not been done so far, to the best of our knowledge. Understandably, the assignments are not straightforward as there are several possible combinations closely matching the band frequencies (see below). On the other hand, the weak peaks at 5767 and 5925 cm^{-1} can be clearly assigned to overtone modes of the symmetric and antisymmetric CH stretching vibrations, respectively. They are slightly lower than twice the fundamental frequencies due to anharmonicity.

In order to shed comprehensive light on the DMSO NIR spectrum, we consider all different possibilities of combining fundamental modes for each combination band. For the 4279 cm^{-1} peak, there are four different possibilities: two different combinations of CH stretching and bending vibrations (2996 + 1310 = 4306 and 2912 + 1407 = 4319) and two combinations of CH stretching with the CSC symmetric and antisymmetric stretching modes (2912 + 667 + 697 = 4276 and 2912 + 2 × 667 = 4246). The latter two possibilities appear to be unlikely at first glance, as they involve three quanta of fundamental modes. On the other hand, the former two would look unlikely as well because they yield a considerable blue-shift with respect to the experimentally observed band. If we consider the DMSO-d_6 spectrum, the combinations of the CD stretching and bending modes would show a large isotopic effect, appearing around 2250 + 757 = 3007 cm^{-1} and 2125 + 820 = 2945 cm^{-1}. The CD/CSC combinations would be found around 2125 + 623 + 612 = 3360 cm^{-1} and 2125 + 2 × 612 = 3349 cm^{-1}. The DMSO-d_6 spectrum shows weak structures at all four positions. Therefore, it is possible that all four combinations above contribute. An illuminating insight can be gained, if we further consider the spectra of aqueous solutions and compare frequency shifts of the fundamental modes and the combination band. As discussed below (Figure 7b), the 4279 cm^{-1} peak exhibits a blue-shift by ∼25 cm^{-1} when the solution contains 95% water. This is well matched by the summed shifts of the combinations, 2912($\Delta\nu$ = 11 cm^{-1}) + 697(9 cm^{-1}) + 667(4 cm^{-1}) and 2996(15 cm^{-1}) + 1310(10 cm^{-1}). Determining the frequency shifts of the CSC stretching modes in the solution IR spectra is challenging due to the interference from the strong water absorption band; hence, an uncertainty of about ±1 cm^{-1}. The results and trends, however, are in line with previous Raman measurements by Noack et al.,[47] where water interference was negligible. The findings are also supported by the DMSO-d_6 solution data. Hence, we can conclude that both combinations may contribute to the band at 4279 cm^{-1}. We expect that the dominant contribution is from the (2996 + 1310) combination because it involves only two modes and thus has a significantly higher probability than the combination of three modes. Again, the combination band frequencies are slightly lower than the sum of the fundamental frequencies due to anharmonicity.

The assignment of the 4397 cm^{-1} band is more straightforward than the 4279 cm^{-1} band because there are only two different possible combinations: 2996 + 1407 = 4403 cm^{-1} and 2996 + 2 × 697 = 4390 cm^{-1}. The wavenumber shift of 17 cm^{-1} when water is added (95% water) is only matched by the combination (2996(15 cm^{-1}) + 1407(1 cm^{-1})), and hence the other possibility is ruled out.

4.2. IR and NIR Spectra of the Binary Solutions. The dominant molecular interaction in aqueous solutions of DMSO is hydrogen-bonding. The primary sites for water−DMSO intermolecular hydrogen bonds (HBs) are the oxygen atom of the DMSO sulfoxide group as an acceptor and the hydrogen atoms of water OH groups as a donor. We thus consider the vibrational signatures of the S═O and O−H groups in detail next.

4.2.1. DMSO SO Stretching Region. Figure 3 displays the concentration-dependent experimental spectra in the SO stretching region. The band between 980 and 1100 cm^{-1} is rich in information, but the interpretation of its complex behavior is not straightforward. As discussed above, in pure DMSO there are four modes in this frequency range, centered at 1019, 1031, 1041, and 1052 cm^{-1}. They correspond to CH_3 rocking and SO stretching modes. As the water content increases, the spectral feature at higher wavenumber (assigned to the SO stretches) reduces in intensity. By contrast, the structure ascribed to the methyl rocking vibrations shows a nonmonotonic behavior. Specifically, the intensity of this structure, initially a shoulder, increases until the water mole fraction reaches about 0.4 and becomes a pronounced peak. As the water concentration further increases, however, it starts to decrease and eventually vanishes. The intriguing behaviors of the entire band are yet to be fully understood, and many studies reported in the literature have apparently avoided analyzing this spectral region in detail. In what follows, we consider a model framework that can offer reasonable explanations for most of the phenomena we and others observed.

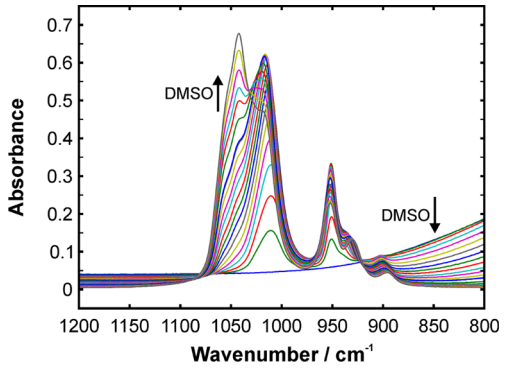

Figure 3. SO stretching band of aqueous DMSO solutions. Different colors are used to make the spectra of different mixture compositions distinguishable.

As mentioned above, the SO stretching modes at 1041 and 1052 cm^{-1} are characteristic of self-associated and non-

DOI: 10.1021/acs.jpcb.5b09196
J. Phys. Chem. B 2015, 119, 14780−14789

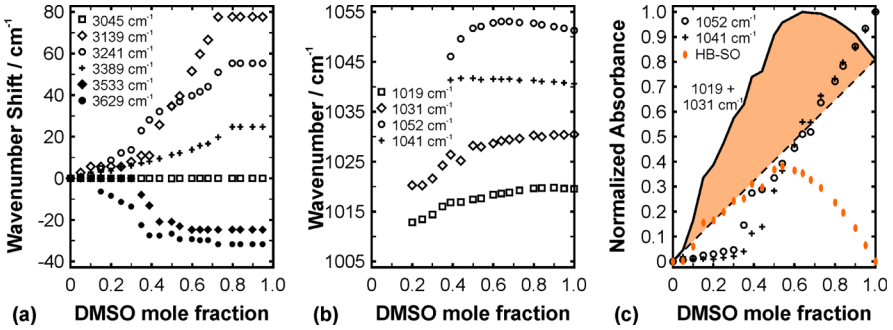

Figure 4. Frequency shifts of (a) the water OH stretching bands and (b) the DMSO SO stretching band as a function of DMSO mole fraction. Panel (c) displays the corresponding intensity changes of the DMSO SO stretching bands.

associated DMSO molecules, respectively. A closer look at the deconvoluted spectra reveals that both contributions show a rather simple behavior when water is added. Figures 4b and 4c show the center frequency and the intensity as a function of DMSO concentration. Starting with pure DMSO, the intensity of both lines decreases linearly until it vanishes at the DMSO mole fraction of around 0.3. This means that the number of "free" and self-associated (incorporated in chain-like and cyclic structures) DMSO molecules decreases systematically upon water addition. At the water mole fraction above 0.7 all DMSO molecules seem to be involved in interactions with water.

It is interesting that, initially, the peak positions remain essentially unchanged when water is added. This indicates that the dipole−dipole interactions are virtually not affected by the water molecules at low and medium concentration. At higher water mole fraction, however, a small red-shift is observed, which means that further water addition to DMSO leads to a gradual weakening of the DMSO−DMSO interactions.

The spectral feature in the low wavenumber region, where the methyl rocking modes are found at 1019 and 1031 cm^{-1} in the pure DMSO case, shows a peculiarity, viz., the intensity enhancement when a small amount of water up to about 30% is admixed (see Figure 4c). The behavior can be explained by the formation of a new species, i.e., water−DMSO dimers with a hydrogen bond between the sulfoxide oxygen and a water hydrogen. As water is added to DMSO, DMSO molecules interacting via the dipole−dipole interactions become replaced by hydrogen-bonded water−DMSO dimers. The hydrogen-bonding interaction of DMSO and water is expected to be stronger than the dipole−dipole interaction between DMSO molecules. Consequently, the SO stretching modes of hydrogen-bonded DMSO are further red-shifted compared to the pure DMSO case. In the aqueous DMSO solutions, it turns out that the frequency of the red-shifted SO stretch coincides with that of the methyl rocking modes. As the IR activity of the stretching mode of the highly polar SO bond is stronger than that of the methyl rocking vibration, the overall intensity of the region around 1020 cm^{-1} increases with the water concentration although the DMSO concentration is reduced. As the DMSO solution is further diluted, the band continues to shift toward lower frequencies, indicating that the hydrogen-bonding network becomes stronger. Around x_{DMSO} = 0.33, an enhanced red-shift is obtained.

For clarity, we mention that we fitted the SO band of aqueous solutions with four Gaussian profiles just like the pure DMSO case. This means that the spectral region corresponding to the overlapping methyl rocking and hydrogen-bonded SO stretching is fitted with two profiles even though, in principle, there can be at least four peaks contributing to the spectrum: the two (weak) methyl rocking modes and the hydrogen-bonded 1DMSO:1water dimer and the 1DMSO:2water trimer. The latter has been identified in previous experimental and computational studies.[1] However, fitting the SO band of the mixture with a total of six Gaussian profiles did not lead to robust and reproducible results. Hence, we decided to use four profiles as in the pure DMSO case with a caveat that additional peaks could make a contribution.

Figure 4c shows another attempt to discriminate between the different contributions, i.e., the methyl rocking modes and the hydrogen-bonded SO stretching modes. The solid line represents the integrated normalized absorbance of the low-frequency wing. As described above, starting from pure DMSO, the intensity initially increases with water addition, which can be attributed to the formation of DMSO−water clusters. Assuming that the methyl groups are not significantly influenced by the molecular interactions with water, we expect that the absorbance of the rocking contributions decreases linearly with decreasing DMSO concentration according to the Beer−Lambert law. This idealized behavior is displayed as the dashed line in Figure 4c. The difference of the actual absorbance (solid line) and the ideal behavior (dashed line) can be attributed to the hydrogen-bonded complexes, which is illustrated as highlighted area. The magnitude of this difference (marked as filled elliptic symbols) suggests that the number of DMSO−water dimers increases until it reaches a maximum around the water mole fraction of 0.5 and then decreases as the water concentration further increases. This is very reasonable in that the highest concentration of such dimers is likely to be attained in the equimolar mixture.

The computational results for vibrational spectra in the low DMSO concentration range are presented in Figure 5. In pure DMSO, the SO stretching mode was found at 1375 cm^{-1} (Figure 1b). In the mixtures, this band shows a slight frequency

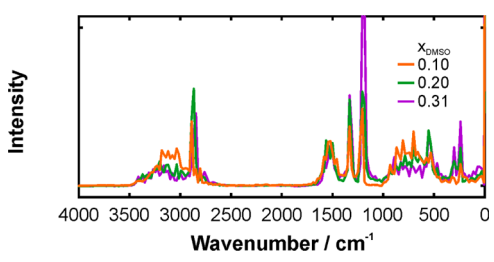

Figure 5. Vibrational spectra of the binary mixtures of water and DMSO obtained from Fourier transformation of the velocity autocorrelation function.

DOI: 10.1021/acs.jpcb.5b09196
J. Phys. Chem. B 2015, 119, 14780−14789

shift and becomes significantly broader (by about a factor of 1.8). This indicates the presence of DMSO molecules in different interaction configurations, which has been suggested by the experimental data as well.

4.2.2. Water OH Stretching Region. Here, we consider the behaviors of the vibrational spectra of DMSO−water mixtures from the point of view of water. Figure 6 displays the

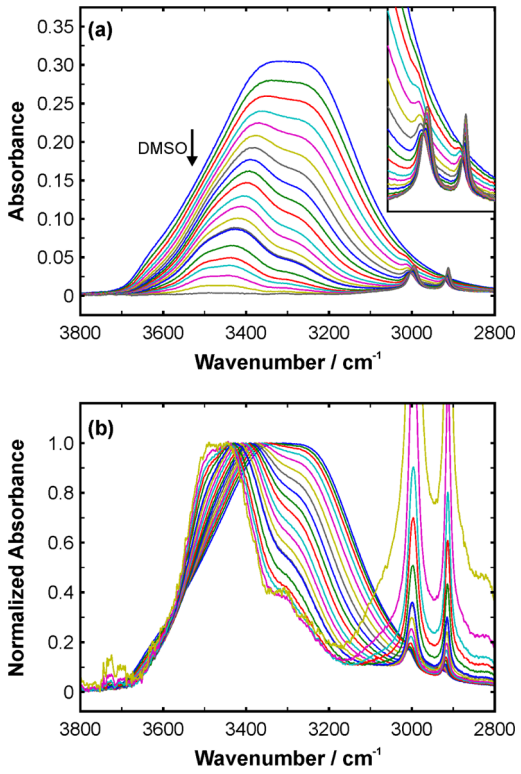

Figure 6. OH stretching band of aqueous DMSO solutions. Panel (a) shows absolute absorbance. The OH band was normalized with respect to the maximum OH absorbance in panel (b). The inset in panel (a) shows the enlarged CH stretching modes of DMSO. Note that the pure DMSO spectrum is omitted in panel (b).

experimental spectra in the OH stretching region. As mentioned above, the pure water band can be deconvolved into six individual Gaussian profiles (see Figure 2): (1) the peak at 3629 cm^{-1} is due to water molecules not participating in hydrogen-bonding interactions; (2) the peak at 3533 cm^{-1} can be attributed to weakly hydrogen-bonded water; (3) the 3389 cm^{-1} mode can be assigned to asymmetrically and the mode (4) at 3241 cm^{-1} to symmetrically hydrogen-bonded water; the low wavenumber component at 3139 cm^{-1} can be assigned to tetracoordinated, fully hydrogen-bonded water. (6) The contribution at 3045 cm^{-1} is not considered in the following discussion. It represents a very broad and low-intensity band compared to the other profiles, and it does not change with mixture composition (see squares in Figure 4a). Hence, it is likely a kind of background rather than a water specific signal.

The spectra of the OH stretching region of the aqueous DMSO solutions are plotted on an absolute absorbance scale in panel (a) of Figure 6, while normalized results with respect to the maximum absorbance value of the OH band are given in panel (b). The latter representation provides a clearer picture of the changes in the band shape. With increasing DMSO concentration, the overall band shows an apparent blue-shift in agreement with the simulated spectra in Figure 5. With the decreasing water content, the overall band becomes narrower and the individual contributions shift in frequency (see Figure 4a). For example, as the water concentration decreases, the shoulder structure at high wavenumber assigned to water molecules not participating in hydrogen-bonding interactions initially shows a red-shift before it stabilizes in wavenumber around the equimolar composition. Above the DMSO mole fractions of 0.5, its frequency essentially does not change with water concentration. A very similar behavior is observed for the second highest frequency mode (i.e., the 3533 cm^{-1} mode in pure water), which is assigned to weakly hydrogen-bonded water. This indicates that the water molecules, which initially are either weakly or not incorporated into the hydrogen-bonding network, interact with DMSO molecules. The red-shifts further suggest that the DMSO−water interactions of these water molecules are stronger than the interactions they are subject to in the pure water.

The other modes of the water OH band show a blue-shift when DMSO is added. This means that the hydrogen-bonding interactions of water molecules that were strongly incorporated in the water HB network become weaker in the mixture. The wavenumber shifts exhibited in Figure 4a show additional interesting behaviors in terms of slope changes. Specifically, the slope changes occur at DMSO mole fractions around x_{DMSO} = 0.33, 0.5, and 0.75, which can be related to the formation of specific molecular configurations and clusters. For instance, the change at the eutectic point x_{DMSO} = 0.33 can be related to a 1DMSO:2water configuration, which has frequently been reported in the literature.[1] 1DMSO:2water clusters have been observed in molecular dynamics simulations[5,48,49] and have been studied in detail by density functional theory methods.[50] For example, Singh et al.[50] suggested a trimer configuration, in which two water molecules each form a hydrogen bond with the oxygen atom of a DMSO molecule, while the water oxygen atoms interact with the methyl hydrogen atoms of the same DMSO molecule. This configuration would mean, if reasonably stable, that the molecular surroundings mainly sees hydrogen atoms at the surface of the cluster. If the mixture at x_{DMSO} = 0.33 favors the formation of such small units with a low tendency to interact with each other, this can provide a molecular-level explanation for the substantial drop of the freezing point observed macroscopically. A liquid consisting of such clusters that barely have directional interactions with their environment will not easily make a phase transition to a frozen state with a crystalline structure.

In the equimolar mixture, the formation of DMSO−water dimers is most likely. This was also suggested by the analysis of the nonideality of the SO band in the previous section (Figure 4c). The most probable formation of 1DMSO:1water complexes is the one with a hydrogen-bond formed between a water hydrogen atom and the sulfoxide oxygen atom. In addition, it is possible that the second water hydrogen interacts with the same sulfoxide oxygen or that the water oxygen interacts with DMSO methyl hydrogen atoms. The latter was also suggested by Dhumal[51] using DFT calculations.

The mixture containing 75% DMSO, where the formation of 3DMSO:1water clusters should be favored, marks another interesting data point in Figure 4a. As the DMSO concentration is raised beyond this point, the individual peaks contributing to the water OH band do not show any further frequency shift. This indicates that the molecular state of water in solution does not change with the addition of DMSO. For x_{DMSO} > 0.75,

DOI: 10.1021/acs.jpcb.5b09196
J. Phys. Chem. B 2015, 119, 14780−14789

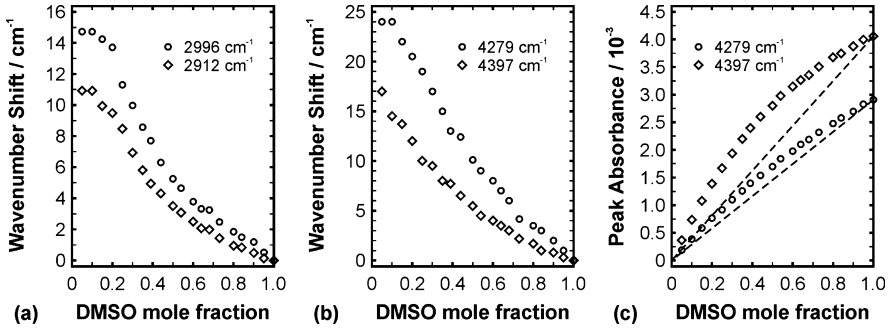

Figure 7. Frequency shifts of (a) the DMSO CH stretching bands and (b) the DMSO combination band as a function of DMSO mole fraction. Panel (c) displays the corresponding intensity changes of the DMSO combination bands. The dashed lines indicate the linear behavior corresponding to the Beer−Lambert law.

virtually all water molecules are involved in interactions solely with DMSO, so that no water molecules interact directly with other water molecules. This can be rationalized as follows: Water has three atoms at which intermolecular interactions can take place. Our results suggest that each atom interacts with one DMSO molecule to form a 3DMSO:1water complex. The water hydrogen atoms can form HBs with sulfoxide oxygen atoms, while the water oxygen atom can engage in a polar interaction with a sulfur atom or form a weak HB with methyl hydrogen atoms of a third DMSO molecule. Because of the large size of DMSO compared to water, such a configuration means that the water molecules are well shielded from each other. In contrast to tetracoordinated molecules in liquid water, the water oxygen atom cannot participate in two interactions here due to steric hindrance. The narrow width of the OH stretching band at high DMSO concentrations lends further support to this hypothesis as a narrow band indicates that the water molecules are in rather well-defined interaction states, i.e., a homogeneous environment.

4.2.3. DMSO CH Vibrations. The previous subsections provided a clear picture of the hydrogen-bonding interactions in aqueous DMSO solutions. In the following, the CH stretching bands in the IR as well as the combination bands in the near-IR are examined. The fundamental stretching modes partly overlap with the broad OH stretching band of water. The enlarged CH peaks are displayed in the inset of Figure 6a. The combination bands observed in the binary solutions are illustrated in Figure S1 of the Supporting Information. The corresponding wavenumber shifts of both the CH stretching modes and combination bands are presented in Figure 7.

The symmetric and antisymmetric CH stretching modes at 2912 and 2996 cm^{-1} shift toward blue when water is added. These results are also noted in the simulated vibrational spectra. The initial degree of the blue-shift, i.e., the slope of the curve starting at pure DMSO in Figure 7, is moderate and almost constant. When the solution contains more than 50% water, the slope becomes considerably steeper before it levels off at x_{DMSO} = 0.1 and below. The combination band in the NIR shows a similar trend, since the stretching mode contributes to the band. The blue-shift indicates that the CH bond becomes stronger upon water addition. The origin of this strengthening may be twofold: (1) the formation of weak hydrogen bonds between water oxygen atoms and methyl hydrogen and (2) the charge redistribution resulting from the formation of strong hydrogen bonds between sulfoxide oxygen and water hydrogen. The small blue-shifts at low water content are attributed mainly to the charge redistribution. This is in line with the previous discussion of the SO and OH vibrations, which suggested the formation of HBs between sulfoxide oxygen and water hydrogen when water is gradually added to DMSO. The enhanced blue shift at x_{DMSO} = 0.5 and below lends support to the aforementioned hypothesis of 1DMSO:2water cluster formation. It is likely that these clusters yield weak hydrogen-bonding interactions between the water oxygen and a methyl group of DMSO. Further evidence in support of this interpretation can be found from the peak absorbance of the combination band in Figure 7c. It shows that the absorbance decreases almost linearly with increasing water concentration until x_{DMSO} = 0.5. This is followed by another linear regime toward zero absorbance but with a considerably different slope. The absorbance is governed by two factors: the concentration of the absorbing species and the IR activity (equivalent to the dipole moment of the vibrating bond). The concentration dependence should be linear according to the Beer−Lambert law, viz., a straight line from the absorbance value at x_{DMSO} = 1 to zero at x_{DMSO} = 0 (dashed lines in Figure 7c), as there is no interference from water absorption. Any deviation from this behavior can be ascribed to changes in the dipole moment. The slope in the range 0.5 < x_{DMSO} < 1 is less steep than the corresponding dashed line, indicating that the dipole moment is enhanced, and the overall effect is an overcompensation of the decrease in concentration. For x_{DMSO} < 0.5 the formation of weak hydrogen bonds exerts an additional influence on the charge distribution. Overall, this leads to counteracting changes in the dipole moment of the CH groups. Such changes in the dipole moment can also be visualized using the excess spectrum, which we turn to next.

4.3. Excess Spectrum. The excess spectrum, defined as the difference between the experimental solution spectrum and its ideal counterpart, is an elegant way of visualizing nonidealities in the position and strength of spectral features. The ideal spectrum is calculated by adding the spectra of the pure substances weighted by their mole fractions. As a consequence, peak shifts manifest as S-shape profiles and changes in the dipole moment lead to negative or positive contributions. When both effects overlap, an asymmetric S-profile may be the result.

Figure 8 illustrates the excess spectra of all the binary solutions we studied as a two-dimensional contour plot. The color map is arranged in such a way that positive excess absorbance is displayed in red while blue represents negative excess absorbance. In other words, red areas indicate an enhanced IR activity and thus an enhanced dipole moment, and

DOI: 10.1021/acs.jpcb.5b09196
J. Phys. Chem. B 2015, 119, 14780−14789

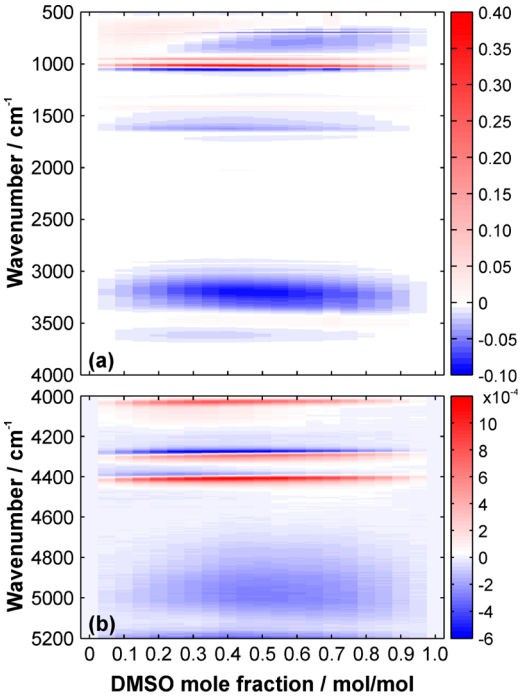

Figure 8. Contour plots of the excess absorbance as a function of wavenumber and DMSO mole fraction. Red features mean positive values, and blue features correspond to negative values.

blue areas mean the opposite. Moreover, combinations of red and blue regions may indicate band shifts. The zoomed-in fingerprint (Figure S2), CH/OH stretching (Figure S3), and NIR (Figure S4) regions with false color representation are provided in the Supporting Information.

In the region of the SO stretching modes of DMSO (~1000 cm^{-1}), red areas can be found on the low wavenumber side, while a blue area is observed on the high wavenumber wing of the band. Both of them can be attributed to the formation of hydrogen-bonded DMSO−water dimers as discussed above. Both features appear to be rather symmetric with respect to a vertical axis at the equimolar composition x_{DMSO} = 0.5. The same is true for the broad blue area in the OH stretching region between 3000 and 3400 cm^{-1}. By contrast, an obviously nonsymmetric shape can be observed around the high-wavenumber wing of the OH stretching band (>3500 cm^{-1}). Absorption in this range was assigned to water molecules either weakly hydrogen-bonded or not participating in hydrogen-bonding interactions. The extreme value (minimum intensity) of this excess feature results at x_{DMSO} = 0.33, the eutectic point. (Figure S5 in the Supporting Information shows two examples of excess absorbance distributions as a function of DMSO mole fraction in order to give an idea of what a symmetric and a nonsymmetric shape look like.) According to the above analysis of the band, the high wavenumber peaks (>3500 cm^{-1}) show a red-shift. Figure 4a reveals that the gradient in the progression of the red-shift is the highest in this concentration range, which explains the behavior observed in the excess plot.

The enlarged spectral region corresponding to the DMSO combination bands is illustrated in panel (b) of Figure 8. While the red areas appear to be symmetric about x_{DMSO} = 0.5, the blue areas do not. The negative excess area just below 4300 cm^{-1} is almost symmetric. It is located where the unperturbed peak at 4279 cm^{-1} appears in the spectrum of pure DMSO. The overall appearance of the red and blue areas in this region suggest quite a symmetric S-shape in the excess spectrum and thus a straightforward peak shift behavior. This is also indicated by the absorbance plotted in Figure 7c, where only minor deviations from the linear relationship were observed. However, the colors around the 4397 cm^{-1} indicate strong nonidealities. Specifically, the red area is rather symmetric while the blue region is highly asymmetric peaking at around x_{DMSO} = 0.3. Furthermore, the intensity of the former is significantly stronger than that of the latter. This may be a result of weak hydrogen bonds forming between water and the methyl groups.

5. SUMMARY AND CONCLUSION

In this paper, we have studied the infrared and near-infrared spectra of the aqueous solutions of dimethyl sulfoxide, which have been the subject of many experimental and theoretical investigations over the years due to their unique properties and important applications. To this end, we performed a detailed analysis of the experimental IR and NIR spectra. The SO and OH stretching regions were evaluated using summed Gaussian profiles. Additionally, the excess spectra were derived as a two-dimensional contour plot as a function of frequency and composition. This plot provides an easily accessible map for visualizing and identifying spectral regions and concentration ranges exhibiting nonideal behavior.

We also performed Car−Parrinello molecular dynamics simulations to obtain computational vibrational spectra at selected mixture compositions. The spectra determined as Fourier transformation of the velocity autocorrelation function yielded reasonable agreement with the experimental results, in particular, for the pure solvents. The simulation reproduces even the complicated shape of the OH stretching band in liquid water, which is a result of the complex hydrogen-bonding network. This is noteworthy as the simulations were run with relatively small numbers of molecules. For pure water, we found that a total of 64 molecules was sufficient to capture virtually all relevant phenomena.

One of the novel aspects of the present work is the special attention paid to the DMSO combination bands in the NIR, which have not been clearly assigned in the literature. With the help of the spectra obtained in the binary solutions and additional measurements in deuterated DMSO, we were able to determine the origin of the combination bands. Combinations of CH stretching and bending modes dominate the bands, but a weak contribution from a combination of CH stretching and symmetric and antisymmetric CSC stretching is likely present in the peak at 4279 cm^{-1}.

In the binary mixtures, the analysis of the SO stretching band provided a semiquantitative picture of the formation and dissociation of hydrogen-bonded DMSO−water complexes. A maximum concentration of these clusters is found in the equimolar mixture. At high DMSO concentration the formation of rather stable 3DMSO:1water complexes is suggested, in which the water is shielded from the surroundings. The formation of 1DMSO:2water trimers, in which the water oxygen atoms interact with the sulfoxide methyl groups, was identified as a possible reason for the strong decrease in the freezing temperature at the eutectic point. This hypothesis is supported by the water and DMSO IR spectra. The DMSO combination bands in the NIR provide further support for the hypothesis that weak hydrogen bonds form at the methyl groups. Hence, this work makes an important step toward understanding the highly nonideal behavior of aqueous DMSO solutions at the eutectic point.

DOI: 10.1021/acs.jpcb.5b09196
J. Phys. Chem. B 2015, 119, 14780−14789

Ongoing and future work will focus on the further exploitation of the potential and the improvement of the accuracy of the computational method in order to obtain a better understanding of the complicated OH frequencies, in particular. This will involve the quantization of the nuclear motion in snapshot structures extracted from the CPMD simulation,[52,53] which will shed further light on the underlying phenomena determining the exciting behavior of DMSO−water mixtures.

■ ASSOCIATED CONTENT

Supporting Information

The Supporting Information is available free of charge on the ACS Publications website at DOI: 10.1021/acs.jpcb.5b09196.

NIR combination bands of aqueous DMSO solutions; enlarged contour plots of the excess absorbance as a function of wavenumber and DMSO mole fraction in the fingerprint region, in the CH/OH stretching region, and in the near-infrared region; excess absorbance at given wavenumber as a function of DMSO mole fraction (PDF)

■ AUTHOR INFORMATION

Corresponding Author

*E-mail: jkiefer@uni-bremen.de (J.K.).

Notes

The authors declare no competing financial interest.

■ ACKNOWLEDGMENTS

This work was supported in part by NSF Grant CHE-1223988 and by EPSRC Grant EP/K00090X/1.

■ REFERENCES

(1) Kiefer, J.; Noack, K.; Kirchner, B. Hydrogen Bonding in Mixtures of Dimethyl Sulfoxide and Cosolvents. *Curr. Phys. Chem.* **2011**, *1*, 340−351.

(2) Palaiologou, M. M.; Molinou, I. E.; Tsierkezos, N. G. Viscosity Studies on Lithium Bromide in Water + Dimethyl Sulfoxide Mixtures at 178.15 and 293.15 K. *J. Chem. Eng. Data* **2002**, *47*, 1285−1289.

(3) Catalán, J.; Díaz, C.; García-Blanco, F. Characterization of Binary Solvent Mixtures of Dmso with Water and Other Cosolvents. *J. Org. Chem.* **2001**, *66*, 5846−5852.

(4) Schichman, S. A.; Amey, R. L. Viscosity and Local Liquid Structure in Dimethyl Sulfoxide-Water Mixtures. *J. Phys. Chem.* **1971**, *75*, 98−102.

(5) Vishnyakov, A.; Lyubartsev, A. P.; Laaksonen, A. Molecular Dynamics Simulations of Dimethyl Sulfoxide and Dimethyl Sulfoxide-Water Mixture. *J. Phys. Chem. A* **2001**, *105*, 1702−1710.

(6) Havemeyer, R. N. Freezing Point Curve of Dimethyl Sulfoxide-Water Solutions. *J. Pharm. Sci.* **1966**, *55*, 851−853.

(7) Rasmussen, D. H.; MacKenzie, A. P. Phase Diagram for the System Water-Dimethylsulfoxide. *Nature* **1968**, *220*, 1315−1317.

(8) Akkok, C. A.; Liseth, K.; Hervig, T.; Ryningen, A.; Bruserud, O.; Ersvaer, E. Use of Different DMSO Concentrations for Cryopreservation of Autologous Peripheral Blood Stem Cell Grafts Does Not Have Any Major Impact on Levels of Leukocyte- and Platelet-Derived Soluble Mediators. *Cytotherapy* **2009**, *11*, 749−760.

(9) Soper, A. K.; Luzar, A. Orientation of Water Molecules around Small Polar and Nonpolar Groups in Solution: A Neutron Diffraction and Computer Simulation Study. *J. Phys. Chem.* **1996**, *100*, 1357−1367.

(10) Mancera, R. L.; Chalaris, M.; Samios, J. The Concentration Effect on the 'Hydrophobic' and 'Hydrophilic' Behaviour around DMSO in Dilute Aqueous DMSO Solutions. A Computer Simulation Study. *J. Mol. Liq.* **2004**, *110*, 147−153.

(11) Kirchner, B.; Hutter, J. Solvent Effects on Electronic Properties from Wannier Functions in a Dimethyl Sulfoxide/Water Mixture. *J. Chem. Phys.* **2004**, *121*, 5133−5142.

(12) Kirchner, B.; Hutter, J. The Structure of a DMSO-Water Mixture from Car-Parrinello Simulations. *Chem. Phys. Lett.* **2002**, *364*, 497−502.

(13) Li, X.; Liu, L.; Schlegel, H. B. On the Physical Origin of Blue-Shifted Hydrogen Bonds. *J. Am. Chem. Soc.* **2002**, *124*, 9639−9647.

(14) Mizuno, K.; Imafuji, S.; Ochi, T.; Ohta, T.; Maeda, S. Hydration of the CH Groups in Dimethyl Sulfoxide Probed by NMR and IR. *J. Phys. Chem. B* **2000**, *104*, 11001−11005.

(15) Mizuno, K.; Kimura, Y.; Morichika, H.; Nishimura, Y.; Shimada, S.; Maeda, S.; Imafuji, S.; Ochi, T. Hydrophobic Hydration of Tert-Butyl Alcohol Probed by NMR and IR. *J. Mol. Liq.* **2000**, *85*, 139−152.

(16) Mrazkova, E.; Hobza, P. Hydration of Sulfo and Methyl Groups in Dimethyl Sulfoxide Is Accompanied by the Formation of Red-Shifted Hydrogen Bonds and Improper Blue-Shifted Hydrogen Bonds: An Ab Initio Quantum Chemical Study. *J. Phys. Chem. A* **2003**, *107*, 1032−1039.

(17) Li, Q.; An, X.; Gong, B.; Cheng, J. Spectroscopic and Theoretical Evidence for the Cooperativity between Red-Shifted Hydrogen Bond and Blue-Shifted Hydrogen Bond in DMSO Aqueous Solutions. *Spectrochim. Acta, Part A* **2008**, *69*, 211−215.

(18) Li, Q.; An, X.; Gong, B.; Cheng, J. Comparison of Contribution of O-H···O═S Hydrogen Bond and C-H···O_w Interaction to the Methyl Blue-shift in Hydration of Dimethyl Sulfoxide. *Vib. Spectrosc.* **2008**, *46*, 28−33.

(19) Li, Q.-Z.; Wang, N.-N.; Yu, Z.-W. Effect of Hydration on the C-H···O Hydrogen Bond: A Theoretical Study. *J. Mol. Struct.: THEOCHEM* **2007**, *847*, 68−74.

(20) Zheng, Y. Z.; He, H. Y.; Zhou, Y.; Yu, Z. W. Hydrogen-Bonding Interactions between [Bmim][BF4] and Dimethyl Sulfoxide. *J. Mol. Struct.* **2014**, *1069*, 140−146.

(21) Li, Q.-Z.; Wang, N.-N.; Zhou, Q.; Sun, S.; Yu, Z. W. Excess Infrared Absorption Spectroscopy and Its Applications in the Studies of Hydrogen Bonds in Alcohol-Containing Binary Mixtures. *Appl. Spectrosc.* **2008**, *62*, 166−170.

(22) Wang, N.-N.; Zhang, Q.-G.; Wu, F.-G.; Li, Q.-Z.; Yu, Z.-W. Hydrogen Bonding Interactions between a Representative Pyridinium-Based Ionic Liquid [Bupy][BF4] and Water/Dimethyl Sulfoxide. *J. Phys. Chem. B* **2010**, *114*, 8689−8700.

(23) Corsetti, S.; Zehentbauer, F. M.; McGloin, D.; Kiefer, J. Characterization of Gasoline/Ethanol Blends by Infrared and Excess Infrared Spectroscopy. *Fuel* **2015**, *141*, 136−142.

(24) Kiefer, J.; Molina Martinez, M.; Noack, K. The Peculiar Nature of Molecular Interactions between an Imidazolium Ionic Liquid and Acetone. *ChemPhysChem* **2012**, *13*, 1213−1220.

(25) Ellis, A.; Zehentbauer, F. M.; Kiefer, J. Probing the Balance of Attraction and Repulsion in Binary Mixtures of Dimethyl Sulfoxide and N-Alcohols. *Phys. Chem. Chem. Phys.* **2013**, *15*, 1093−1096.

(26) Zehentbauer, F. M.; Kiefer, J. Molecular Solution Behaviour of an Intermediate Biofuel Feedstock: Acetone-Butanol-Ethanol (ABE). *ChemPhysChem* **2015**, DOI: 10.1002/cphc.201500835.

(27) Thomas, M.; Brehm, M.; Fligg, R.; Vöhringer, P.; Kirchner, B. Computing Vibrational Spectra from Ab Initio Molecular Dynamics. *Phys. Chem. Chem. Phys.* **2013**, *15*, 6608−6622.

(28) Gaigeot, M. P. Theoretical Spectroscopy of Floppy Peptides at Room Temperature. A DFTMD Perspective: Gas and Aqueous Phase. *Phys. Chem. Chem. Phys.* **2010**, *12*, 3336−3359.

(29) Bernasconi, M.; Silvestrelli, P. L.; Parrinello, M. Ab Initio Infrared Absorption Study of the Hydrogen-Bond Symmetrization in Ice. *Phys. Rev. Lett.* **1998**, *81*, 1235−1238.

(30) Vener, M. V.; Sauer, J. Environmental Effects on Vibrational Proton Dynamics in H5O2+: DFT Study on Crystalline H5O2+ClO4−. *Phys. Chem. Chem. Phys.* **2005**, *7*, 258−263.

(31) Bursulaya, B. D.; Kim, H. J. Spectroscopic and Dielectric Properties of Liquid Water: A Molecular Dynamics Simulation Study. *J. Chem. Phys.* **1998**, *109*, 4911−4919.

DOI: 10.1021/acs.jpcb.5b09196
J. Phys. Chem. B 2015, 119, 14780−14789

(32) Car, R.; Parrinello, M. Unified Approach for Molecular Dynamics and Density-Functional Theory. *Phys. Rev. Lett.* **1985**, *55*, 2471−2474.
(33) Hutter, J.; Ballone, P.; Bernasconi, M.; Focher, P.; Fois, E.; Goedecker, S.; Marx, D.; Parrinello, M.; Tuckerman, M. E. Cpmd Version 3.17.1, Max Planck Institut fuer Festkoerperforschung Stuttgart and IBM Zurich Research Laboratory, Stuttgart and Zurich.
(34) Becke, A. D. Density-Functional Exchange-Energy Approximation with Correct Asymptotic Behavior. *Phys. Rev. A: At., Mol., Opt. Phys.* **1988**, *38*, 3098−3100.
(35) Lee, C.; Yang, W.; Parr, R. G. Development of the Colle-Salvetti Correlation-Energy Formula into a Functional of the Electron Density. *Phys. Rev. B: Condens. Matter Mater. Phys.* **1988**, *37*, 785−789.
(36) Troullier, N.; Martins, J. L. Efficient Pseudopotentials for Plane-Wave Calculations. *Phys. Rev. B: Condens. Matter Mater. Phys.* **1991**, *43*, 1993−2006.
(37) Sprik, M.; Hutter, H.; Parrinello, M. Ab Initio Molecular Dynamics Simulation of Liquid Water: Comparison of Three Gradient- Corrected Density Functionals. *J. Chem. Phys.* **1996**, *105*, 1142.
(38) Grimme, S. Accurate Description of Van Der Waals Complexes by Density Functional Theory Including Empirical Corrections. *J. Comput. Chem.* **2004**, *25*, 1463−1473.
(39) Klemenkova, Z. S.; Kononova, E. G. Elucidation of the Water-DMSO Mixing Process Based on a IR Study. *J. Solution Chem.* **2015**, *44*, 280−292.
(40) Bertoluzza, A.; Bonora, S.; Battaglia, M. A.; Monti, P. Raman and Infrared Study on the Effects of Dimethylsulfoxide (DMSO) on Water Structure. *J. Raman Spectrosc.* **1979**, *8*, 231−235.
(41) Kiefer, J.; Frank, K.; Schuchmann, H. P. Attenuated Total Reflection Infrared (ATR-IR) Spectroscopy of a Water-in-Oil Emulsion. *Appl. Spectrosc.* **2011**, *65*, 1024−1028.
(42) Schmidt, D. A.; Miki, K. Structural Correlations in Liquid Water: A New Interpretation of IR Spectroscopy. *J. Phys. Chem. A* **2007**, *111*, 10119−10122.
(43) Fawcett, W. R.; Kloss, A. A. Solvent-Induced Frequency Shifts in the Infrared Spectrum of Dimethyl Sulfoxide in Organic Solvents. *J. Phys. Chem.* **1996**, *100*, 2019−2024.
(44) McLain, S. E.; Soper, A. K.; Luzar, A. Orientational Correlations in Liquid Acetone and Dimethyl Sulfoxide: A Comparative Study. *J. Chem. Phys.* **2006**, *124*, 074502.
(45) Rao, B. G.; Singh, U. C. A Free Energy Perturbation Study of Solvation in Methanol and Dimethyl Sulfoxide. *J. Am. Chem. Soc.* **1990**, *112*, 3803−3811.
(46) Shikata, T.; Sugimoto, N. Reconsideration of the Anomalous Dielectric Behavior of Dimethyl Sulfoxide in the Pure Liquid State. *Phys. Chem. Chem. Phys.* **2011**, *13*, 16542−16547.
(47) Noack, K.; Kiefer, J.; Leipertz, A. Concentration Dependent Hydrogen Bonding Effects on the Dimethyl Sulfoxide Vibrational Structure in the Presence of Water, Methanol and Ethanol. *ChemPhysChem* **2010**, *11*, 630−637.
(48) Vaisman, I. I.; Berkowitz, M. L. Local Structural Order and Molecular Associations in Water-DMSO Mixtures. Molecular Dynamics Study. *J. Am. Chem. Soc.* **1992**, *114*, 7889−7896.
(49) Luzar, A.; Chandler, D. Structure and Hydrogen Bond Dynamics of Water-Dimethyl Sulfoxide Mixtures by Computer Simulations. *J. Chem. Phys.* **1993**, *98*, 8160−8173.
(50) Singh, S.; Srivastava, S. K.; Singh, D. K. Raman Scattering and DFT Calculations Used for Analyzing the Structural Features of DMSO in Water and Methanol. *RSC Adv.* **2013**, *3*, 4381−4390.
(51) Dhumal, N. R. Electronic Structure, Molecular Electrostatic Potential and Hydrogen Bonding in DMSO-X Complexes (X = Ethanol, Methanol and Water). *Spectrochim. Acta, Part A* **2011**, *79*, 654−660.
(52) Breka, M. Z.; Wójcik, M. J.; Boczar, M.; Witek, L.; Yasuda, M.; Ozaki, Y. Car-Parrinello Molecular Dynamics Simulations of Infrared Spectra of Crystalline Vitamin C with Analysis of Double Minimum Proton Potentials for Medium-Strong Hydrogen Bonds. *J. Phys. Chem. B* **2015**, *119*, 7922−7930.
(53) Stare, J.; Mavri, J.; Grdadolnik, J.; Zidar, J.; Maksić, Z. B.; Vianello, R. Hydrogen Bond Dynamics of Histamine Monocation in Aqueous Solution: Car-Parrinello Molecular Dynamics and Vibrational Spectroscopy Study. *J. Phys. Chem. B* **2011**, *115*, 5999−6010.

DOI: 10.1021/acs.jpcb.5b09196
J. Phys. Chem. B 2015, 119, 14780−14789